Influence of the Pt→Ag Donor−Acceptor Bond and Polymorphism on the Spectroscopic and Optical Properties of Heteropolynuclear Benzoquinolateplatinum(II) Complexes

Juan Forniés,* Susana Ibáñez, Antonio Martín, and Manuel Sanz

Departamento de Química Inorgánica, Instituto de Ciencia de Materiales de Aragón, Universidad de Zaragoza-CSIC, 50009 Zaragoza, Spain

Jesús R. Berenguer, Elena Lalinde,* and Javier Torroba

Departamento de Química, Grupo de Síntesis Química de La Rioja, UA-CSIC, Universidad de La Rioja, 26006, Logroño, Spain

Received May 23, 2006

A new cyclometalated derivative, $(NBu_4)[Pt(bzq)(C_6Cl_5)_2]$ (**2**) (bzq = 7,8-benzoquinolate), and three novel polymetallic species containing donor−acceptor Pt→Ag bonds, $(NBu_4)[\{Pt(bzq)(C_6F_5)_2\}_2Ag]$ (**3**) and $[\{Pt(bzq)(C_6X_5)_2\}Ag(PPh_3)]$ (X = F (**4**), Cl (**5**)), have been synthesized and characterized by X-ray diffraction methods. **3** is prepared by reaction of $(NBu_4)[Pt(bzq)(C_6F_5)_2]$ (**1**) with $AgClO_4$ in 1:1 or 1:0.5 molar ratio, while **4** and **5** are the results of the reaction of the corresponding $(NBu_4)[Pt(bzq)(C_6X_5)_2]$ (X = F (**1**), Cl (**2**)) precursors with $[Ag(OClO_3)(PPh_3)]$ in 1:1 molar ratio. **3** has been found to crystallize in two forms: monoclinic (**3a**) and triclinic (**3b**), which differ not only in the conformation of the basic Pt_2Ag anion (*anti* and planar **3a**, staggered and nonplanar **3b**), but also in the crystal packing ($\pi\cdots\pi$ extended structure **3a**, and a stacked dimer **3b**) and luminescence at 298 K (orange **3a**, green **3b**). At 77 K, the orange band (568 nm) of **3a**, attributed to a $\pi\pi^*$ excimeric emission, is not detected, and both polymorphs exhibit identical green emission (^{3}LC/^{3}MLCT). Spectroscopic study of **4** and **5** (UV−vis and luminescence) was also performed to examine the role of the Pt→Ag donor−acceptor bond. The most significant feature is the blue shift observed in the low-energy UV absorption and the appearance of two, close, distinct, structured emissions with short (487 **4**; 490 nm **5**) and long (502 nm **4**, **5**) lifetime, but only in the solid state at 77 K.

Introduction

Square-planar platinum(II) cyclometalated complexes represent an important class of compounds that possess interesting photophysical and photochemical properties, with potential application in chemosensing and optoelectronic devices.[1−20] These complexes have also been investigated as luminescent probes for biomolecular targets, such as DNA and proteins,[19,21−23] and liquid crystal optical storage materials.[24] Many of these complexes are photoluminescent, and previous investigations have shown that the emissive state arises from intraligand ($^3\pi\pi^*$), metal-to-ligand charge transfer (^{3}MLCT), ligand field (^{3}LF), and, even, ^{3}LL′CT. The nature of the emissive state is found to be sensitive to both the cyclometalated and the ancillary ligands and can be systematically tuned by the variation of the ligands coordinated to the Pt(II) central ion. Of particular interest in these studies is the occurrence of weak noncovalent Pt···Pt[2,10,25,26] or $\pi\cdots\pi$[6,7,13] interactions, which are found to give

(1) Ma, B.; Djurovich, P. I.; Thompson, M. E. *Coord. Chem. Rev.* **2005**, *249*, 1501, and references therein.
(2) Wong, W. Y.; He, Z.; So, S. K.; Tong, K. L.; Lin, Z. *Organometallics* **2005**, *24*, 4079.
(3) Jude, H.; Baver, J. A. K.; Connick, W. B. *Inorg. Chem.* **2005**, *44*, 1211, and references therein.
(4) Pérez, S.; López, C.; Caubet, A.; Bosque, R.; Solans, X.; Bardía, M. F.; Roig, A.; Molins, E. *Organometallics* **2004**, *23*, 224, and references therein.
(5) Chin, B. K. W.; Lam, M. H. W.; Lee, D. Y. K.; Wong, W. Y. *J. Organomet. Chem.* **2004**, *689*, 2888.
(6) Lu, W.; Chan, M. C. W.; Zhu, N.; Che, C. M.; Li, C.; Hui, Z. *J. Am. Chem. Soc.* **2004**, *126*, 7639.
(7) Díez, A.; Forniés, J.; García, A.; Lalinde, E.; Moreno, M. T. *Inorg. Chem.* **2005**, *44*, 2443.
(8) Fernández, S.; Forniés, J.; Gil, B.; Gómez, J.; Lalinde, E. *Dalton Trans.* **2003**, 822.
(9) Williams, J. A. G.; Beeby, A.; Davies, E. S.; Weinstein, J. A.; Wilson, C. *Inorg. Chem.* **2003**, *42*, 8609.
(10) Lai, S. W.; Lam, M. H. W.; Lu, W.; Cheung, K. K.; Che, C. M. *Organometallics* **2002**, *21*, 226.
(11) Yersin, H.; Donges, D.; Humbs, W.; Strasser, J.; Sitters, R.; Glasbeek, M. *Inorg. Chem.* **2002**, *41*, 4915.
(12) Lu, W.; Mi, B. X.; Chan, M. C. W.; Hui, Z.; Zhu, N.; Lee, S. T.; Che, C. M. *Chem. Commun.* **2002**, 206.
(13) Yam, V. W.; Tang, R. P. L.; Wong, K. M. C.; Lu, X. X.; Cheung, K. K.; Zhu, N. *Chem. Eur. J.* **2002**, *8*, 4066.
(14) Brooks, J.; Babayan, Y.; Lamansky, S.; Djurovich, P. I.; Tsyba, I.; Bau, K.; Thompson, M. E. *Inorg. Chem.* **2002**, *41*, 3055.
(15) Jolliet, P.; Gianini, M.; von Zelewsky, A.; Bernadinelly, G.; Stoekli-Evans, H. *Inorg. Chem.* **1996**, *35*, 4889.
(16) De Priest, J.; Zheng, G. Y.; Goswami, N.; Eichhorn, D. M.; Woods, C.; Rillema, D. P. *Inorg. Chem.* **2000**, *39*, 1955.
(17) Balashev, K. P.; Puzyk, M. V.; Koflyar, V. S.; Kulinova, M. V. *Coord. Chem. Rev.* **1997**, *159*, 109.
(18) Chassot, L.; von Zelewsky, A. *Inorg. Chem.* **1987**, *26*, 2814.
(19) Wong, K. H.; Chan, M. C. W.; Che, C. M. *Chem. Eur. J.* **1999**, *5*, 2845.
(20) Zheng, G. Y.; Rillema, D. P.; De Priest, J.; Woods, C. *Inorg. Chem.* **1998**, *37*, 3588.
(21) Zheng, G. Y.; Rillema, D. P. *Inorg. Chem.* **1998**, *37*, 1392.
(22) Wu, L. Z.; Cheung, T. C.; Che, C. M.; Cheung, K. K.; Lam, M. H. W. *Chem. Commun.* **1998**, 1127.
(23) Che, C. M.; Yang, M.; Wong, K. H.; Chan, H. L.; Lam, W. *Chem. Eur. J.* **1999**, *5*, 3350.
(24) Buey, J.; Díez, L.; Espinet, P.; Kitzerow, H. S.; Miguel, J. A. *Chem. Mater.* **1996**, *8*, 2375.

10.1021/om0604526 CCC: $33.50
Publication on Web 08/04/2006

low-energy triplet emissions (MMLCT d$\sigma^*\rightarrow\pi^*$ and excimeric ligand-to-ligand $\pi-\pi^*$) that are particularly sensitive to the microenvironment, a property that is essential for molecular recognition. Many investigations have been focused on mononuclear platinum complexes and, occasionally, on bi- and triplatinum systems,[3,5−7,10,25−27] paying particular attention to the role of Pt···Pt and $\pi\cdots\pi$ stacking interactions in the luminescent properties. In view of the remarkable effect of Pt−Pt interaction on the spectroscopic and photophysical properties of this type of complexes, we were interested to know if the electronic structures of the complexes could also be affected by other Pt−M bonding interactions. We were particularly interested in understanding the effects of the formation of donor−acceptor Pt→M bonds on the electronic structures.

In the course of our research we have developed synthetic methods for the preparation of complexes containing Pt→M donor−acceptor bonds.[28−34] Our success with these preparations has mainly been based on the use of perhalophenyl platinate(II) complexes. Cyclometalating ligands such as 2-phenylpyridine (Hphpy) or 2-(2-thienyl)pyridine (Hthpy) are also known to enhance the electron-donating ability of Pt(II), allowing the formation of Pt→M bonds, even with neutral substrates of the type [Pt(C∼N)$_2$] (C∼N = C, N cyclometalating ligand).[35−37] Recently, we have reported the synthesis of (NBu$_4$)[Pt(bzq)(C$_6$F$_5$)$_2$] (**1**) (bzq = 7,8-benzoquinolate), and we have demonstrated that the anionic fragment [Pt(bzq)(C$_6$F$_5$)$_2$]$^-$ is a useful entity to form the bimetallic cationic complex [{Pt(bzq)(C$_6$F$_5$)$_2$}Cd(cyclen)]$^+$ through a Pt→Cd bond.[38] We observed that coordination of [Cd(cyclen)]$^{2+}$ to the [Pt(bzq)(C$_6$F$_5$)$_2$]$^-$ unit has an impact upon the energy emission, which was attributed to an admixture of triplet dπ(Pt)→π^*(bzq) (MLCT) and $\pi\pi^*$ (IL) transitions. Upon formation of the Pt→Cd bond, a substantial blue shift was observed in relation to the precursor, in either the absorption or emission spectra.

In this paper, we report the synthesis of a related anionic derivative, (NBu$_4$)[Pt(bzq)(C$_6$Cl$_5$)$_2$] (**2**), and the results of the reactivity of both anionic precursors [Pt(bzq)(C$_6$X$_5$)$_2$]$^-$ (X = F (**1**), Cl (**2**)) toward the Ag(I) ion. We describe the preparation of a new trimetallic complex, (NBu$_4$)[{Pt(bzq)(C$_6$F$_5$)$_2$}$_2$Ag] (**3**), which crystallizes in two different polymorphs (**3a** and **3b**), and the effects of two bimetallic neutral Pt→Ag bonds upon the spectroscopic properties of the precursors (**1**, **2**) and the properties of both polymorphs have been examined.

Scheme 1

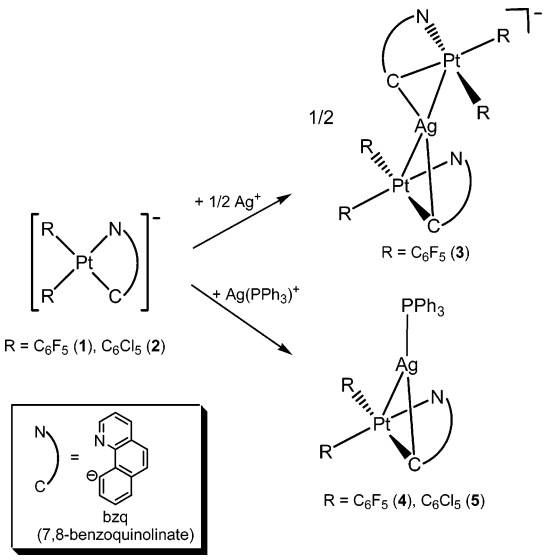

Results and Discussion

Reaction of [NBu$_4$][Pt(bzq)(C$_6$X$_5$)$_2$] with AgClO$_4$. Preparation of [NBu$_4$][{Pt(bzq)(C$_6$F$_5$)$_2$}$_2$Ag] (3). Reaction of [NBu$_4$][Pt(bzq)(C$_6$F$_5$)$_2$] (**1**) with AgClO$_4$ (0.5 or 1 equiv) in acetone (see Scheme 1) proceeds with an immediate change of the color of the solution from colorless to pale yellow. After the usual workup to eliminate NBu$_4$ClO$_4$ (see Experimental Section), only an oily residue was obtained. Slow diffusion of *n*-hexane into a saturated solution of this residue in acetone yields crystals with a yellowish appearance. Careful observation reveals that there are two types of crystals, with different crystal habits (blocks and plates), which at room temperature display distinct orange (**3a**) or green (**3b**) luminescence under UV light (see below). The structures (X-ray) of both crystals indicated the formation of two polymorphs of the complex [NBu$_4$][{Pt(bzq)(C$_6$F$_5$)$_2$}$_2$Ag] (**3**), which crystallizes in the monoclinic (**3a**) or triclinic (**3b**) system, respectively. A similar procedure with the pentachlorophenyl analogue [NBu$_4$][Pt(bzq)(C$_6$Cl$_5$)$_2$] also leads to an oily residue, but unfortunately, in this case, we were not able to isolate a definite product.

The crystal structures of the two polymorphs of **3** (monoclinic **3a** and triclinic **3b**) have been determined by X-ray diffraction. Views of the corresponding anions of both polymorphs, **3a** and **3b**, are shown in Figure 1, and selected interatomic distances and angles are given in Table 1. Both polymorphs **3a** and **3b** contain two square-planar "Pt(bzq)(C$_6$F$_5$)$_2$" moieties with a silver atom sandwiched between them and connected by two Pt→Ag bonds. As shown by Figures 1a and 1b, one of the most important differences within the anion is the relative disposition of the two "Pt(bzq)(C$_6$F$_5$)$_2$" fragments. Thus, while in **3a** they adopt an "alternated" or *anti* position (Figure 2a), and are almost parallel (dihedral angle 6.1(2)°), in **3b** one of the C$_6$F$_5$ groups bound to Pt(1) (C(1)) is directly located over a C$_6$F$_5$ group bound to Pt(2) (C(32)) and the Pt coordination planes form a dihedral angle of 30.3(1)° (see Figure 2b). In addition, the separation between the two Pt atoms is 5.055(1) Å in **3a** and 5.299(1) Å in **3b**.

The intermetallic distances (Pt(1), Pt(2)−Ag = 2.7584(5), 2.6843(5) Å for **3a**; Pt(1), Pt(2)−Ag = 2.7018(4), 2.6897(4) Å for **3b**) are in the lower region of the range known for Pt→Ag

(25) Lai, S. W.; Chan, C. W.; Cheung, K. K.; Peng, S. M.; Che, C. M. *Organometallics* **1999**, *18*, 3991.
(26) Lai, S. W.; Chan, C. W.; Cheung, K. K.; Che, C. M. *Organometallics* **1999**, *18*, 3327.
(27) Ma, B.; Li, J.; Djurovich, P. I.; Yousufuddin, M.; Bau, R.; Thompson, M. E. *J. Am. Chem. Soc.* **2005**, *127*, 28.
(28) Forniés, J.; Martín, A. In *Metal Clusters in Chemistry*; Braunstein, P., Oro, L. A., Raithby, P. R., Eds.; Wiley-VCH: Weinheim, 1999; Vol. 1, p 417.
(29) Casas, J. M.; Falvello, L. R.; Forniés, J.; Gómez, J.; Rueda, A. J. *J. Organomet. Chem.* **2000**, *593−594*, 421.
(30) Ara, I.; Falvello, L. R.; Forniés, J.; Sicilia, V.; Villarroya, P. *Organometallics* **2000**, *19*, 3091.
(31) Falvello, L. R.; Forniés, J.; Martín, A.; Sicilia, V.; Villarroya, P. *Organometallics* **2002**, *21*, 4604.
(32) Ara, I.; Falvello, L. R.; Forniés, J.; Gómez, J.; Lalinde, E.; Merino, R. I.; Usón, I. *J. Organomet. Chem.* **2002**, *663*, 284.
(33) Ara, I.; Forniés, J.; Sicilia, V.; Villarroya, P. *Dalton Trans.* **2003**, 4238.
(34) Alonso, E.; Forniés, J.; Fortuño, C.; Martín, A.; Orpen, A. G. *Organometallics* **2003**, *22*, 5011.
(35) Yamaguchi, T.; Yamazaki, F.; Ito, T. *J. Am. Chem. Soc.* **1999**, *121*, 7405.
(36) Yamaguchi, T.; Yamazaki, F.; Ito, T. *J. Am. Chem. Soc.* **2001**, *123*, 743.
(37) Janzen, D. E.; Mehne, L. F.; VanDerveer, D. G.; Grant, G. J. *Inorg. Chem.* **2005**, *44*, 8182.
(38) Forniés, J.; Ibáñez, S.; Martín, A.; Gil, B.; Lalinde, E.; Moreno, M. T. *Organometallics* **2004**, *23*, 3963.

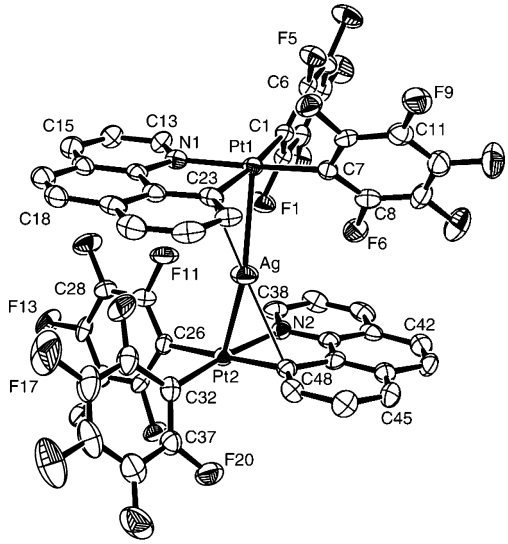

a

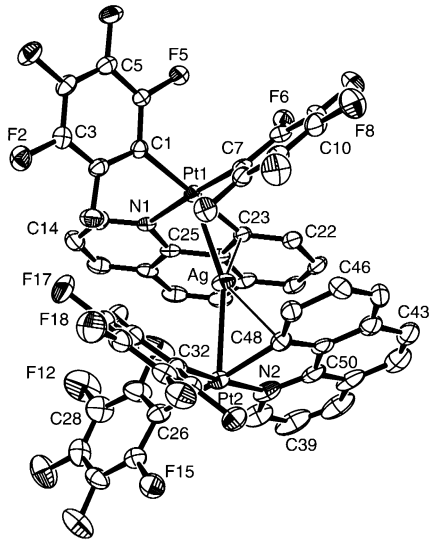

b

Figure 1. View of the molecular structure of the anion of complex $[NBu_4][\{Pt(bzq)(C_6F_5)_2\}_2Ag]$ as found in the monoclinic **3a** (a) or the triclinic **3b** (b) polymorphs. Ellipsoids are drawn at the 50% probability level. Hydrogen atoms are omitted for clarity.

donor acceptor bonds.[28] The Pt(1)−Ag−Pt(2) angle is 136.49(2)° in **3a** and more linear in **3b** (158.77(2)°). This means that the Pt−Ag lines are not perpendicular to the best square environments of the Pt atoms (the angles are 34.5(1)° for Pt(1) and 24.5(1)° for Pt(2) in **3a** and 33.9(1)° and 24.4(1)°, respectively, in **3b**). It seems that in both polymorphs the silver atom leans to the less crowded area, avoiding the proximity of the bulky C_6F_5 groups (no short *o*-F···Ag contacts are found), and contacts (η^1-type) with the metalated C atoms of the bzq ligands (Ag−C(23) = 2.420(6) Å in **3a** and 2.418(5) Å in **3b**, Ag−C(48) = 2.626(6) Å in **3a** and 2.538(5) Å in **3b**) in such a way that the shorter Ag−C distance correlates with the longer Pt−Ag one. Silver is known to have a remarkable affinity for some aromatic π-donor systems.[39−52] The η^1 and η^2 coordination

Table 1. Selected Bond Lengths (Å) and Angles (deg) for the Monoclinic (3a) and Triclinic (3b) Polymorphs of $[NBu_4][\{Pt(bzq)(C_6F_5)_2\}_2Ag]$

	3a	3b
Pt(1)−Ag	2.7584(5)	2.7018(4)
Pt(2)−Ag	2.6843(5)	2.6897(4)
Pt(1)−C(1)	2.065(6)	2.075(5)
Pt(1)−C(7)	2.019(6)	2.003(5)
Pt(1)−C(23)	2.060(6)	2.066(5)
Pt(1)−N(1)	2.086(5)	2.093(4)
Pt(2)−C(26)	2.083(6)	2.072(5)
Pt(2)−C(32)	2.016(7)	2.007(5)
Pt(2)−C(48)	2.043(6)	2.051(5)
Pt(2)−N(2)	2.097(5)	2.100(5)
Ag−C(23)	2.420(6)	2.418(5)
Ag−C(48)	2.626(6)	2.538(5)
C(1)−Pt(1)−C(7)	87.9(2)	87.4(2)
C(7)−Pt(1)−C(23)	97.9(3)	95.7(2)
C(23)−Pt(1)−N(1)	80.7(2)	81.0(2)
C(1)−Pt(1)−N(1)	93.4(2)	96.0(2)
C(26)−Pt(2)−C(32)	88.4(3)	91.8(2)
C(32)−Pt(2)−C(48)	94.4(3)	92.9(2)
C(48)−Pt(2)−N(2)	80.7(2)	80.8(2)
C(26)−Pt(2)−N(2)	96.4(2)	94.5(2)
C(23)−Ag−C(48)	156.1(2)	129.3(2)
Pt(1)−Ag−Pt(2)	136.49(2)	158.77(2)

modes are found to be the most usual, with the Ag−C lines almost perpendicular to the plane of the aromatic rings, which are frequently arranged in parallel layers in the crystal structure.[39,44] In complexes **3a** and **3b**, the aromatic ring forms part of the bzq ligand that is bonded to Pt, and as a consequence, the Ag−C lines are not perfectly perpendicular to the corresponding aromatic ring, but form angles in the range 22.8(1)−30.5(1)° with the corresponding bzq planes. These η^1-Ag−C interactions are important and, along with the Pt→Ag bonds, clearly contribute to fulfillling the electron requirements of the acidic Ag(I) center. The final bonding interaction of Ag(I) to the Pt−C(orthometalated) bond in both polymorphs (**3a** and **3b**) is comparable to that recently reported by Ito and co-workers[36] in the infinite helical cationic chain $[\{Pt(phpy)_2\}_2\{Ag(Me_2CO)\}_2]_n^{2n+}$ and in the discrete cation $[\{Pt(thpy)_2\}_3\{Ag(Me_2CO)\}_2]^{2+}$ (Pt−Ag 2.6746(7)−2.8121(9) Å; η^1-Ag−C(aromatic) 2.354(10)−2.558(7) Å). Four additional complexes containing M−Ag bonds and similar η^1-Ag−C(aromatic) interactions have been reported: $[Pd(L)(H_2O)Ag(SO_3CF_3)]^+$ (L = 5,8,11-trioxa-2,14-dithia(15)-*m*-cyclophane; Pd−Ag = 2.884 Å, Ag−C = 2.395 Å);[53] $[PdAg(C_6H_4\text{-}o\text{-}CH_2NMe_2)(PPh_2NOMe)]_n$ (Pd−Ag = 2.884 Å, Ag−C = 2.264 Å);[54] $[Au(mesityl)(PPh_3)Ag(\mu\text{-}SC_4H_8)]_2^{2+}$ (Au−Ag = 2.824 Å, Ag−C = 2.327 Å);[55] and $[\{Au(mesityl)(AsPh_3)\}_2Ag]^+$ (Au−Ag = 2.777 Å, Ag−C =

(39) Munakata, M.; Wu, L. P.; Ning, G. L.; Kuroda-Sowa, T.; Maekawa, M.; Suenaga, Y.; Maeno, N. *J. Am. Chem. Soc.* **1999**, *121*, 4968.
(40) Zhong, J. C.; Munakata, M.; Kuroda-Sowa, T.; Maekawa, M.; Suenaga, Y.; Konaka, H. *Inorg. Chem.* **2001**, *40*, 3191.
(41) Wen, M.; Maekawa, M.; Munakata, M.; Suenaga, Y.; Kuroda-Sowa, T. *Inorg. Chim. Acta* **2002**, *338*, 111.
(42) Munakata, M.; Wu, L. P.; Kuroda-Sowa, T.; Maekawa, M.; Suenaga, Y.; Ohta, T.; Konaka, H. *Inorg. Chem.* **2003**, *42*, 2553.
(43) Munakata, M.; Zhong, J. C.; Kuroda-Sowa, T.; Maekawa, M.; Suenaga, Y.; Kasahara, M.; Konaka, H. *Inorg. Chem.* **2001**, *40*, 7078.
(44) Munakata, M.; Wu, L. P.; Kuroda-Sowa, T.; Maekawa, M.; Suenaga, Y.; Ning, G. L.; Kojima, T. *J. Am. Chem. Soc.* **1998**, *120*, 8610.
(45) Liu, S. Q.; Kuroda-Sowa, T.; Konaka, H.; Suenaga, Y.; Maekawa, M.; Mizutani, T.; Ning, G. L.; Munakata, M. *Inorg. Chem.* **2005**, *44*, 1031.
(46) Falvello, L. R.; Forniés, J.; Martín, A.; Sicilia, V.; Villarroya, P. *Organometallics* **2002**, *21*, 4604.
(47) Dong, Y.-B.; Geng, Y.; Ma, J.-P.; Huang, R.-Q. *Inorg. Chem.* **2005**, *44*, 1693.
(48) Dong, Y.-B.; Jin, G.-X.; Zhao, X.; Tang, B.; Huang, R.-Q.; Smith, M. D.; Stitzer, K. E.; zur Loye, H.-C. *Organometallics* **2004**, *23*, 1604.
(49) Dong, Y.-B.; Zhao, X.; Jin, G.-X.; Huang, R.-Q.; Smith, M. D. *Eur. J. Inorg. Chem.* **2003**, 4017.
(50) Cote, A. P.; Shimizu, G. K. H. *Inorg. Chem.* **2004**, *43*, 6663.
(51) Brasey, T.; Buryak, A.; Scopelliti, R.; Severin, K. *Eur. J. Inorg. Chem.* **2004**, 964.
(52) Munakata, M.; Wu, L. P.; Ning, G. L. *Coord. Chem. Rev.* **2000**, *198*, 171.
(53) Kickham, J. E.; Loeb, S. J. *Organometallics* **1995**, *14*, 3584.

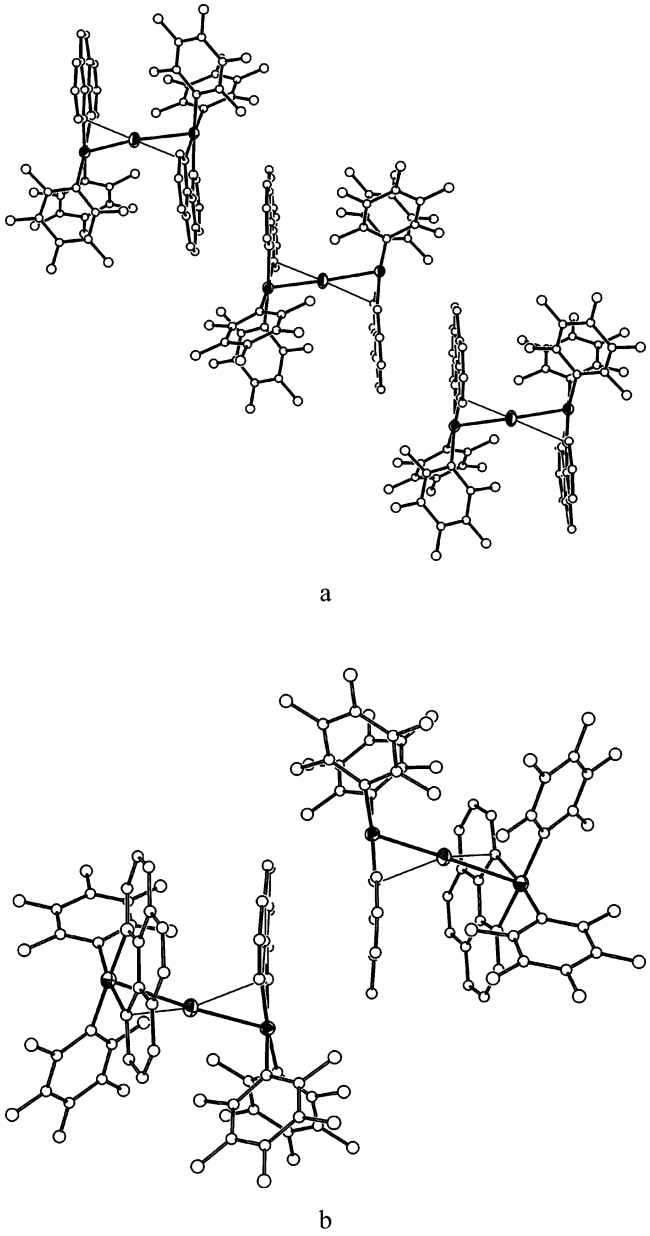

Figure 2. Supramolecular arrangement of the anions of complex $[NBu_4][\{Pt(bzq)(C_6F_5)_2\}_2Ag]$, showing the different disposition of the square Pt planes: (a) monoclinic polymorph **2a**; (b) triclinic polymorph **2b**.

2.272 Å).[56] It is important to point out that in these systems the σ nature of the Pt−C_{ipso} bond of the ligand containing the aromatic ring is clear, and the geometry of the complexes excludes any other possibility of a three-center two-electron M(μ-C_{ipso})Ag bond, which is a well-known bond type that has been found in some polynuclear silver complexes.[57,58]

The conformational polymorphism observed in the anion **3** is intriguing. In principle, the alternated disposition found in **3a** seems to be the most adequate in order to avoid the steric repulsions caused by the bulky pentafluorophenyl groups, but the fact that complex **3** also crystallizes in a nonalternate structure, such as that found in **3b**, indicates that the energy difference between both configurations is not large. The small differences in the analogous bond lengths in **3a** and **3b**, mainly those in which the silver atom is involved, which seem to be slightly shorter in **3b**, are compensated by a significant difference in the final packing of the anions in the lattice (Figure 2). Thus, as is shown in Figure 2a, in **3a** the anions are arranged in such a way that the N(1) bzq plane is parallel to the N(2) bzq plane of a neighboring anion, resulting in an infinite stacking of anions related by $\pi-\pi$ interactions (∼3.6 Å).[6,7,13,59−61] In contrast, in **3b**, these π interactions (∼3.6 Å) are located only within the N(1) bzq planes of two adjacent anions, giving rise to a π-stacked dimer (see Figure 2b). These $\pi-\pi$ stackings are among the most important weak interactions[6,7,13,59−61] and, along with hydrogen bonding, dominate the development of modern supramolecular chemistry,[39,42−44] having a prominent role in molecular recognition and self-assembly processes, such as the packing of aromatic molecules or fragments in the crystalline state. Although polymorphism is a phenomenon that is fairly common in organic systems,[62] well-established examples involving organometallic compounds,[63] especially organoplatinum derivatives, remain scarce.[64−69]

Crystals of **3a** and **3b** are indistinguishable by NMR spectroscopy. The ^{1}H NMR spectrum (CD_2Cl_2) of crystals of **3** shows the signals corresponding to the bzq ligand and NBu_4^+ integration in the expected ratio. The ^{19}F NMR spectrum shows that all the fluorine atoms are nonequivalent, and eight signals, partially overlapped, are observed in the *o*-F region. The spectrum at −90 °C does not change substantially. On the other hand, the ^{19}F NMR spectrum in acetone-d_6 at room temperature exhibits two broad signals in the *ortho* fluorine region with platinum satellites, and two complex signals at a higher field comprising one *para* and two *meta* fluorines each, thus indicating the existence of some sort of dynamic processes.

Reaction of $[NBu_4][Pt(bzq)(C_6X_5)_2]$ with $[Ag(OClO_3)(PPh_3)]$. Preparation of $[\{Pt(bzq)(C_6X_5)_2\}Ag(PPh_3)]$ (X = F (4), Cl (5)). Reaction of $[NBu_4][Pt(bzq)(C_6X_5)_2]$ with $[Ag(OClO_3)(PPh_3)]$ in 1:1 molar ratio yields, after elimination of NBu_4ClO_4, the neutral complexes $[\{Pt(bzq)(C_6X_5)_2\}Ag(PPh_3)]$ (X = F (**4**), Cl (**5**)) as yellow solids (see Scheme 1). Complexes **4** and **5** have been characterized by usual analytical and spectroscopic means, and their structures confirmed by X-ray crystallography (see Experimental Section). The $^{31}P\{^1H\}$ NMR spectra ($CDCl_3$) show the expected signal corresponding to the PPh_3 ligand as two doublets, due to coupling of the phosphorus atom to the ^{107}Ag and ^{109}Ag nuclei (51.8% and 48.2% relative abundance, respectively). In both complexes, the signal also

(54) Braunstein, P.; Frison, C.; Oberbeckmann-Winter, N.; Morise, X.; Messaoudi, A.; Benard, M.; Rohmer, M.-M.; Welter, R. *Angew. Chem., Int. Ed.* **2004**, *43*, 6120.
(55) Contel, M.; Jiménez, J.; Jones, P. G.; Laguna, A.; Laguna, M. *J. Chem. Soc., Dalton Trans.* **1994**, 2515.
(56) Contel, M.; Garrido, J.; Gimeno, M. C.; Jones, P. G.; Laguna, A.; Laguna, M. *Organometallics* **1996**, *15*, 4939.
(57) Tyrra, W.; Wickleder, M. S. *Z. Anorg. Allg. Chem.* **2002**, *628*, 1841.
(58) Meyer, E. M.; Gambarotta, S.; Floriani, C.; Chiesi-Villa, A.; Guastini, C. *Organometallics* **1989**, *8*, 1067.
(59) Hunter, C. A.; Sanders, J. K. M. *J. Am. Chem. Soc.* **1990**, *112*, 5525.
(60) Hunter, C. A. *Chem. Soc. Rev.* **1994**, 101.
(61) Farley, S. J.; Rochester, D. L.; Thompson, A. L.; Howard, J. A. K.; Williams, J. A. *Inorg. Chem.* **2005**, *44*, 9690.
(62) Desiraju, G. R., Ed. *Organic Solid State Chemistry*; Elsevier Science Publishing: New York, 1987.
(63) Braga, D.; Grepioni, F. *Chem. Soc. Rev.* **2000**, *29*, 229.
(64) Bennet, B. L.; Ruddick, D. M. *Inorg. Chem.* **1996**, *35*, 4703.
(65) Connick, W. B.; Marsh, R. E.; Schaefer, W. P.; Gray, H. B. *Inorg. Chem.* **1997**, *36*, 913.
(66) Charmant, J. P. H.; Forniés, J.; Gómez, J.; Lalinde, E.; Merino, R. I.; Moreno, M. T.; Orpen, A. G. *Organometallics* **1999**, *18*, 3353, and references therein.
(67) Stork, J. R.; Olmstead, M. M.; Balch, A. L. *J. Am. Chem. Soc.* **2005**, *127*, 6512.
(68) Yam, V. W.; Yu, K. L.; Cheung, K. K. *J. Chem. Soc., Dalton Trans.* **1999**, 2913.
(69) Bai, D. R.; Wang, S. *Organometallics* **2006**, *25*, 1517.

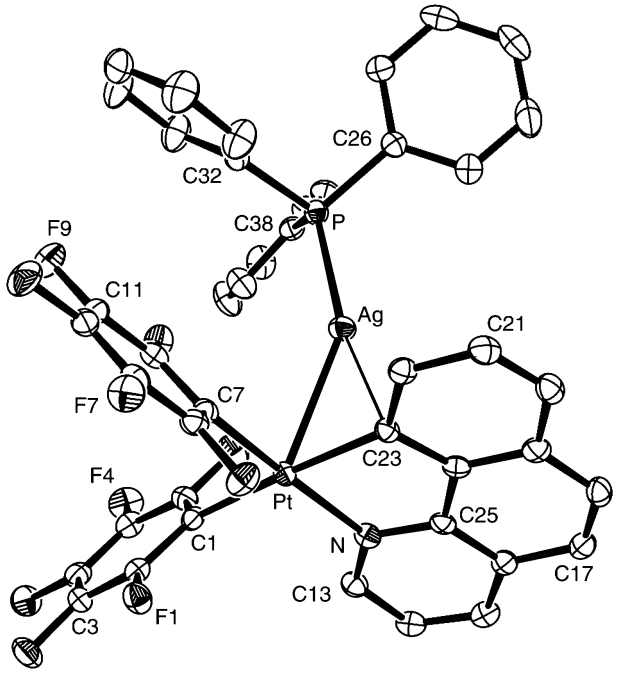

a

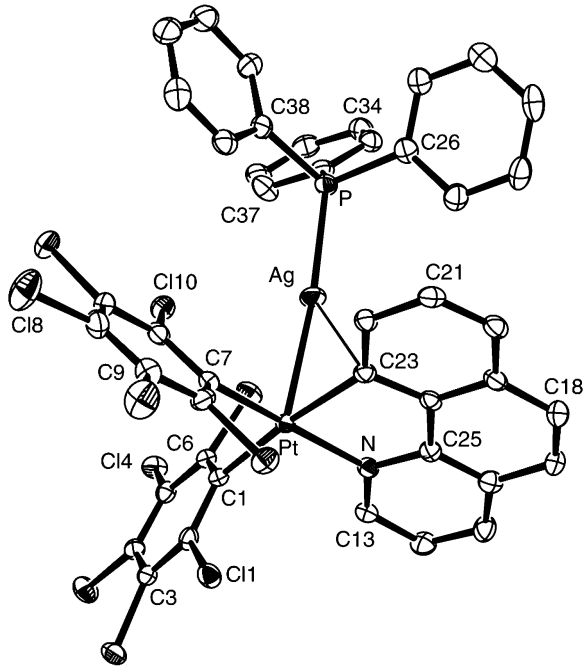

b

Figure 3. View of the molecular structure of complexes [{Pt(bzq)-$(C_6F_5)_2$}Ag(PPh_3)]·$CHCl_3$·0.5*n*-C_6H_{14} (**4**·$CHCl_3$·0.5*n*-C_6H_{14}) and [{Pt(bzq)$(C_6Cl_5)_2$}Ag(PPh_3)]·0.58$CHCl_3$·0.25*n*-C_6H_{14} (**5**·0.58$CHCl_3$·0.25*n*-C_6H_{14}).

shows ^{195}Pt satellites ($^2J(^{195}Pt-P)$ = 228 Hz, **4**; 236 Hz, **5**), confirming the persistence of the Pt−Ag bond in solution.

The ^{19}F NMR of **4** at room temperature reveals the presence of two types of C_6F_5 groups, with typical AA′MM′X spin systems, indicating that the Pt coordination is a symmetry plane. As the $^{31}P\{^1H\}$ NMR spectrum confirms the presence of the Pt−Ag bond in solution, the equivalence of the two *o*-F of the same group probably takes place by rotation of the C_6F_5 ligands around the Pt−C_{ipso} bonds. Curiously, upon cooling, only one of these signals broadens and, finally, splits into two different resonances at −60 °C, thus indicating that, at this temperature, the rotation of one of the C_6F_5 groups is slow enough on the NMR time scale. The other signal remains almost unaltered during the cooling process. The different energetic barriers to the rotation around both Pt−C(*ipso*) bonds have been previously related to the different size of the mutually *cis* donor atoms to the C_6F_5 groups.[70] In this complex, the interaction of the Pt−C(orthometalated) bond to the Ag(I) center probably generates a "bulkier" donor fragment close to the C_6F_5 mutually *cis* to this carbon atom, giving rise to a higher barrier to the rotation of this group. The rotation of the C_6F_5 *cis* to the small N atom could be fast enough on the NMR time scale, even at low temperature.

Table 2. Selected Bond Lengths (Å) and Angles (deg) for [{Pt(bzq)$(C_6F_5)_2$}Ag(PPh_3)]·$CHCl_3$·0.5*n*-C_6H_{14} (4**·$CHCl_3$·0.5*n*-C_6H_{14}) and [{Pt(bzq)$(C_6Cl_5)_2$}Ag(PPh_3)]·0.58$CHCl_3$·0.25*n*-C_6H_{14} (**5**·0.58$CHCl_3$·0.25*n*-C_6H_{14})**

	4·$CHCl_3$·0.5*n*-C_6H_{14}	**5**·0.58$CHCl_3$·0.25*n*-C_6H_{14}
Pt−C(1)	2.072(3)	2.087(5)
Pt−C(7)	2.010(3)	2.033(5)
Pt−C(23)	2.062(3)	2.074(5)
Pt−N	2.084(3)	2.093(4)
Pt−Ag	2.7227(3)	2.6748(5)
Ag−P	2.3466(10)	2.3731(13)
Ag−C(23)	2.352(3)	2.556(4)
C(1)−Pt−C(7)	89.2(1)	94.4(2)
C(7)−Pt−C(23)	96.3(1)	93.3(2)
C(23)−Pt−N	80.7(1)	81.2(2)
C(1)−Pt−N	94.0(1)	91.2(2)
P−Ag−C(23)	165.37(9)	134.20(11)
P−Ag−Pt	145.24(3)	173.53(4)

Drawings of the molecular structures of both complexes (**4**, **5**), confirming the formation of Pt→Ag bonds, are shown in Figure 3 (see also Table 2). The Pt−Ag distances (2.7227(3) Å in **4** and 2.6748(5) Å in **5**) are similar to those found in **3** and, again, in the lower region of the range known for this kind of bond.[28] The bzq ligand is almost coplanar with the platinum square plane in both derivatives (dihedral angle 3.4(1)° in **4** and 9.6(1)° in **5**). The two complexes also show η^1-Ag−C interactions. Thus, the Pt−Ag lines are inclined toward the C(orthometalated) C(23) of the bzq ligand, the angle with the perpendicular to the Pt plane being 34.9(1)° in **4** and 27.2(1)° in **5**. The steeper inclination in complex **4** (Ag−Pt−C(23) angle of 56.9(1)° in **4** vs 63.7(2)° in **5**) leads to shorter Ag−C(23) (2.352(3) Å for **4** vs 2.557(5) Å for **5**), suggesting that the η^1-Ag−C interaction is stronger in the pentafluorophenyl complex **4**, and this inversely correlates with the strength of the Pt−Ag bonds, as indicated by their lengths. Given the relatively short Ag−C(23) distance found in **4**, the Ag−C(22) is also relatively short, 2.679(4) Å (cf. 3.019(5) Å in **5**), but this is most likely a result of the proximity of Ag and C(22) rather than a possible η^2-Ag−C system. The inclination of the silver centers toward the bzq ligand causes its separation from the pentahalophenyl ligands in such a way that in **4** the closest fluorine atom is located more than 3.17 Å away from the silver center, and thus no *o*-F···Ag contacts are present. In complex **5**, the closest Cl atom (Cl(10)) is at 2.990(1) Å from Ag. This greater proximity is caused by the geometry around the silver center in **5** and the bigger size of the Cl with respect to the F. In both complexes, the silver atom completes its coordination with a PPh_3 ligand, the Pt−Ag−P array being almost linear in **5** (173.53(4)° vs 145.24(3)° in **4**, probably due to steric effects caused by the presence of the bulkier C_6Cl_5 ligands.

(70) Casares, J. A.; Espinet, P.; Martínez-Ilarduya, J. M.; Lin, Y. S. *Organometallics* **1997**, *16*, 770.

Table 3. Absorption Data (5×10^{-5} M Solutions) for Complexes 1−5

compound	absorption/nm ($10^3\,\epsilon/M^{-1}\,cm^{-1}$)
$[NBu_4][Pt(bzq)(C_6F_5)_2]$ (**1**)	243(66.4), 260(58.4), 315(27.15), 345(20.1), 380(12.1), 425(6.9) (*CH_2Cl_2*)
$[NBu_4][Pt(bzq)(C_6Cl_5)_2]$ (**2**)	219sh(18.8), 236(60.4), 260(39.9), 290sh(17.0), 309(15.2), 350(7.5), 407(3.9), 444sh(1.7) (*CH_2Cl_2*) 215(55.4), 233(63.7), 258sh(39.1), 291(17.1), 311(15.0), 346(7.4), 400(3.6), 438(1.2) (*acetonitrile*)
$[NBu_4][\{Pt(bzq)(C_6F_5)_2\}_2Ag]$ (**3**)	216sh(15.6), 232(47.1), 254(36.3), 309(14.6), 354(8.1), 376(5.1), 426(2.7) (*CH_2Cl_2*) 215(56.2), 233(64.6), 256(56.9), 286sh(20.8), 306(19.1), 343(12.1), 383(6.3), 426(2.7) (*acetonitrile*)
$[\{Pt(bzq)(C_6F_5)_2\}Ag(PPh_3)]$ (**4**)	221sh(19.2), 239(62.0), 278sh(27.4), 311(15.9), 340(8.2), 365(4.8), 413(3.4) (*CH_2Cl_2*) 222(57.4), 241sh(48.0), 256(42.6), 279sh(15.4), 303(10.3), 344(5.2), 389(2.6), 423(1.1) (*acetonitrile*)
$[\{Pt(bzq)(C_6Cl_5)_2\}Ag(PPh_3)]$ (**5**)	221sh(19.4), 239(63.5), 277sh(24.3), 310(12.5), 344(6.1), 420(2.5) (*CH_2Cl_2*) 214(55.2), 232(62.0), 256sh(42.6), 277sh(21.0), 307(12.3), 348(5.4), 400(2.9), 425(1.5) (*acetonitrile*)

Table 4. Photophysic Data for Complexes 1−5 in the Solid State and in 10^{-3} M CH_2Cl_2 Solutions

compound	(*T*/K)	λ_{em}/nm	τ/μs
$[NBu_4][Pt(bzq)(C_6F_5)_2]$ (**1**)	solid (298)	518	16.5[a]
	solid (77)	514, 550, 595sh	
	CH_2Cl_2 (298)	[b]	
	CH_2Cl_2 (77)	490, 526, 567, 611sh	
$[NBu_4][Pt(bzq)(C_6Cl_5)_2]$ (**2**)	solid (298)	500sh, 538max, 570	6.8
	solid (77)	496, 536max, 577, 620	18
	CH_2Cl_2 (298)	[c]	
	CH_2Cl_2 (77)	495max, 532, 577, 620	
$[NBu_4][\{Pt(bzq)(C_6F_5)_2\}_2Ag]$ (**3**)	crystalline solid (298)[d]	510,[e] 534,[e] 572max[f]	
	crystalline solid (77)[g]	512max, 551, 590	11.5−15.4[d]/10.7−13.9[h]
	CH_2Cl_2 (298)	506, 541max	
	CH_2Cl_2 (77)	504max, 538, 585	
$[\{Pt(bzq)(C_6F_5)_2\}Ag(PPh_3)]$ (**4**)	solid (298)	491max, 523, 562sh	12.4
	solid (77)	487•, 502+, 520•, 540,+ 585+	12.4 at 487 nm [∼278(45%), ∼13.6(55%)][i]
	CH_2Cl_2 (77)	495max, 530, 570, 625 sh	
$[\{Pt(bzq)(C_6Cl_5)_2\}Ag(PPh_3)]$ (**5**)	solid (298)	491max, 524, 563sh	11.4
	solid (77)	490•, 502max+, 525•, 543+, 586sh	∼21.2 at 490 nm [∼206 (66%), ∼26.0 (34%)][i]
	CH_2Cl_2 (77)	490max, 525, 560	

[a] Measured in KBr pellets at 298 K. [b] A very weak emission is detected at ca. 520 nm. [c] A very weak emission at ca. 550 nm. [d] Initial crystalline mixture of **3a** and **3b** obtained by diffusion of *n*-hexaxe into solutions of **3** in acetone. [e] Due to polymorph **3b**. [f] Due to polymorph **3a**. [g] Mixture of **3a** and **3b** or nearly pure **3a**. [h] Nearly pure crystalline **3a**. [i] Measurements in the low-energy peaks.

It is interesting to note that both bimetallic complexes **4** and **5** establish weak $\pi-\pi$ interactions (3.4−3.5 Å in **4**, 3.7−3.8 Å in **5**) in such a way that the bzq ligands of two neighboring complexes stack, forming dimers in a similar way to polymorph **3b** (Figure 2b).

It is noteworthy to compare the structures of complexes **4** and **5** with that of the related, previously reported complex $[\{Pt(bzq)(C_6F_5)_2\}Cd(cyclen)](ClO_4)$.[38] In this complex the Pt−Cd distance (2.688(1) Å) is similar to the Pt−Ag distances found in **4** and **5**, but the Pt−Cd line leans only slightly toward the 7,8-benzoquinolate ligand (angle with the perpendicular to the Pt coordination 17.6(2)°) excluding any Cd···C(bzq) interaction.

Electronic and Luminescence Spectroscopy. The absorption and emission spectra, and other photophysical data, are summarized in Tables 3 and 4. For comparative purposes, the data of the precursor complex **1** are also included. The anionic precursors **1** and **2** exhibit high-energy bands, whose intensity and shapes are typical of ligand-centered transitions (^{1}LC, C_6F_5, bzq) somewhat perturbed by platinum coordination (range 243−380 nm for **1** and 219−407 for **2**). In addition, both complexes show a lowest energy absorption peak (located at 425 and 444 nm in **1** and **2**, respectively), which, in accordance with similar assignments,[2,3,7,9,10,17,27] is assigned to a ^{1}MLCT (5d(Pt)→p*(bzq)). The presence of the highly electron-withdrawing C_6F_5 ligands, which will tend to decrease the energy of the dπ(Pt) orbitals, could be responsible for the blue shift observed in **1** in relation to **2**. The most significant feature of the bimetallic neutral Pt−Ag complexes (**4** and **5**), in which, as commented above, the Pt−Ag donor−acceptor bond is present in solution, is that the low-energy peak is clearly blue-shifted in relation to the corresponding precursors (CH_2Cl_2, 413 nm in **4** and 420 nm in **5**; see Figure 4). This fact, previously observed in $[Pt(bzq)(C_6F_5)_2Cd(Cyclen)]ClO_4$ (λ^{max}_{abs} 410 nm),[38] is consistent with the formation and presence in solution of the Pt−Ag donor−acceptor bond, which produces an increase in the electrophilicity

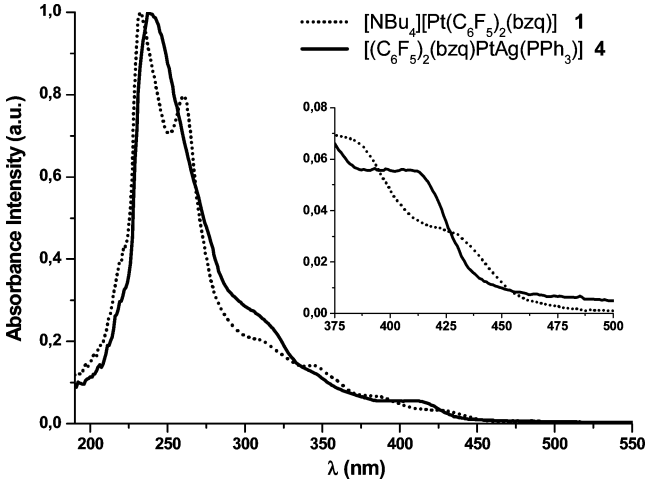

Figure 4. Absorption spectra of complexes **1** and **4** in CH_2Cl_2 (5.0×10^{-5} M) at room temperature.

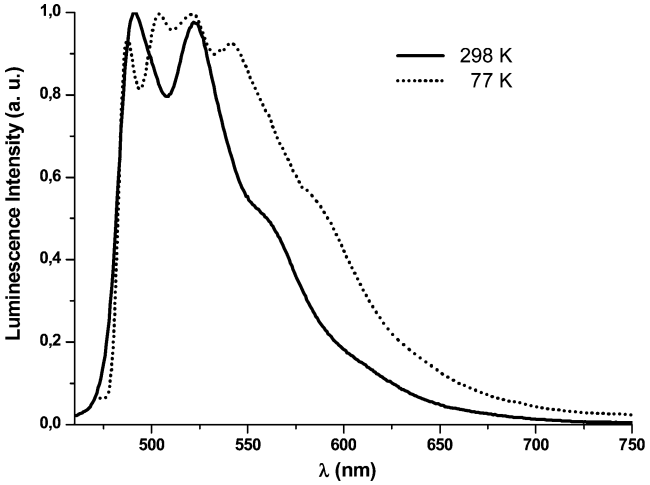

Figure 5. Emission spectra of complex **4** in the solid state at different temperatures (λ_{exc} = 420 nm).

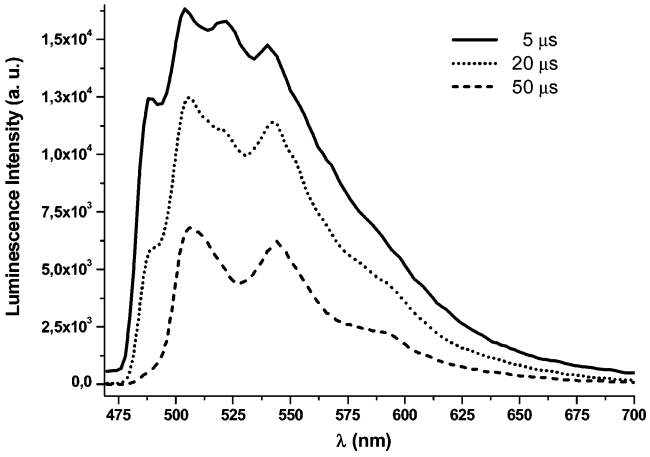

Figure 6. Emission spectra with different delays of complex **4** in the solid state at 77 K (λ_{exc} = 420 nm).

of the Pt metal center, resulting in a blue shift for the MLCT absorption. In contrast to this behavior, in the trinuclear Pt_2Ag anionic complex **3**, in which the silver centers connect two anionic entities, the lowest energy absorption occurs at 426 nm. The similarity of this value (and also the whole spectrum) to that of the precursor **1** suggests that, probably, its integrity is, at least partially, broken in solution, liberating the anionic fragment $[Pt(bzq)(C_6F_5)_2]^-$ to some extent.

All complexes are brightly emissive in the solid state and in glassy solutions and are virtually nonemissive in CH_2Cl_2 solution (see bottom of Table 4) at 298 K, except complex **3**, for which a weak emission is detected with maxima at 506 and 541 nm. As in complex **1**,[38] the pentachlorophenyl anionic derivative **2** exhibits, in the solid state at room temperature, a slightly asymmetric emission, which becomes well structured at 77 K and in glass (CH_2Cl_2, 77 K). In glassy CH_2Cl_2 solution (77 K), the emission in complex **2** is slightly red-shifted relative to that observed for **1** (λ_{max} 495 nm in **2** vs 490 nm in **1**), but in the solid state at 77 K, the emission in complex **1** is found at 514 nm vs 496 nm in **2**. The observed emission lifetimes (in the microsecond range) and structured luminescence are consistent with an emission originating from a mixed ^{3}LC/^{3}MLCT excited state. The heterobimetallic complex derivatives **4** and **5** are comparatively better emitters than the corresponding precursors and exhibit a well-resolved vibronic band even in the solid state at room temperature. Interestingly, the emission profile and emission maxima (λ_{max} 491, 524, 563(sh) nm in **5** vs 491, 523, 562 nm in **4**) are identical for both complexes, and the measurements of the lifetime, which fits well to only one component (τ 12.4 μs in **4** vs 11.4 μs in **5**), are also rather similar, suggesting a similar emissive state that presumably has, in these systems, a primarily ^{3}IL parentage. Comparable structured emissions with λ_{max} at 495 nm for **4** and 490 nm for **5** are also observed in frozen CH_2Cl_2 (77 K), with only minor differences from the corresponding precursor (490 nm in **1**, 495 nm in **2**) (see Figure S1 in the Supporting Information (SI)), pointing to a negligible influence of the Pt−Ag bond in the emissive state. The most significant difference from the precursors is detected for both complexes in the solid state at 77 K. To illustrate this point, the spectra of complex **4** in the solid state are shown in Figure 5 (see also Figure S2 in the SI for complex **5**). Upon cooling, two close, structured bands with different emission origins at 487 and 502 nm for **4** and at 490 and 502 nm for **5** are clearly resolved. The emissions with different delays are shown in Figure 6 for complex **4** (Figure S3 in the SI for complex **5**). As can be observed, the structured emission with peak maxima at 487 and 520 nm has a shorter lifetime, and after 50 μs, only the low-energy emission with peak maxima at 502, 540, and 585 nm is observed. Lifetime measurements registered at the high-energy peak in both complexes fit to only one component (τ 12.4 μs for **4**, ∼21.2 μs for **5**), while, as expected, in the low-energy peaks a long and a short component are always obtained (τ ∼278, ∼13.6 μs for **4**; ∼206, ∼26 μs for **5**). The short component is attributed in both complexes to the presence of the structured high-energy emission. The structured (∼1400 cm^{-1}) low-energy and long-lived emission appears at 502 nm in both complexes, being tentatively attributed to a $^3\pi\pi^*$ emissive state with intraligand character (^{3}LC). The structured (∼1300 cm^{-1} in **4**, ∼1360 cm^{-1} in **5**) high-energy emission, which is slightly blue-shifted in relation to the corresponding precursor (487 nm in **4** vs 514 nm in **1**; 490 nm in **5** vs 496 nm in **2**), reflecting the formation of the Pt−Ag donor−aceptor bond, is assigned to a ^{3}MLCT or a mixed ^{3}IL/^{3}MLCT manifold. At low temperature in the solid state, the formation of the Pt−Ag donor−aceptor bond probably slows down the intersystem crossing rate between the emissive states.

In fluid CH_2Cl_2 solution, the trinuclear anion complex **3** exhibits a structured emission (506, 541 nm), which becomes well structured at 77 K (504(max), 538, 585 nm) and slightly red-shifted in relation not only to the precursor **1** but also to the remaining heterometallic complexes (495 nm in **4**, 490 nm in **5**). The observed intense green emission is independent of the complex concentration and excitation wavelength, suggesting the absence of any low-energy excimeric emission due to inter- or intramolecular $\pi-\pi$ interactions in frozen solution. As previously commented, upon diffusion of *n*-hexane into an acetone solution of **3**, two crystals forms, **3b** and **3a** (see Figure 1 for the X-ray analyses), that exhibit different visible yellowish-green and orange luminescence, respectively, were obtained. Unfortunately, we have been able to separate only a few crystals of nearly pure polymorph **3a** in order to record the corresponding luminescence spectra (298, 77 K). The spectrum of complex **3a** and that of the mixture of crystals (**3a**, **3b**) generated from acetone/*n*-hexane in the solid state at 298 K are shown in Figure 7. Complex **3a** exhibits a broad low-energy band with a maximum at 572 nm. This emission is comparable to that observed for other platinum complexes exhibing $\pi-\pi$ interactions[6,10,13] and is therefore assigned to a $\pi\pi^*$ excimeric emission, in agreement with the fact that this polymorph exhibits an extended aggregation in the solid, dominated by a relatively

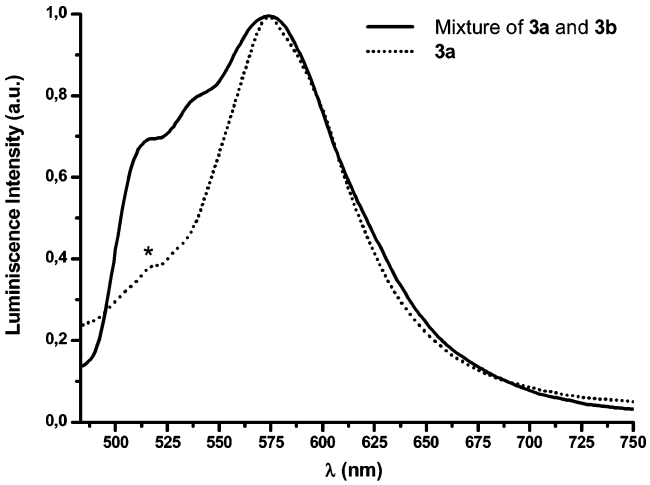

Figure 7. Emission spectra of nearly pure **3a** (* denotes small impurity of brigthly emissive polymorph **3b**) and the initial crystalline mixture of **3a** and **3b** in the solid state at room temperature (λ_{exc} = 430 nm).

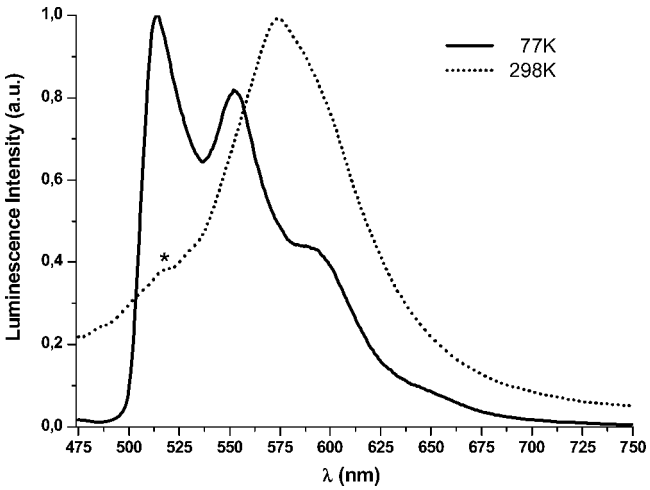

Figure 8. Emission spectra of nearly pure **3a** (* denotes small impurity of brightly emissive polymorph **3b**) in the solid state at 298 and 77 K (λ_{exc} = 430 nm).

short intermolecular $\pi-\pi$ interaction between the bzq ligands. Moreover, the mixture of crystals (**3a**, **3b**) exhibits a high-energy vibronic emission, with maxima slightly red-shifted to that observed in frozen CH_2Cl_2 solution (510, 534 solid at 298 K vs 504, 538, 585 CH_2Cl_2 at 77 K), which is therefore attributed to the polymorph form **3b**. Interestingly, upon cooling to 77 K, the luminescence of both (nearly pure **3a** and the mixture **3a**/**3b**) becomes visually more intense and is seen with a greenish appearance. The emission is similar for **3b**, but is clearly blue-shifted for **3a** (Figure 8), showing only a highly structured emission (512(max), 551, 590 nm), typical of luminescence from states of primarily ^{3}LC with a certain degree of metal-to-ligand charge transfer (^{3}MLCT). The orange emission, which seems to be a characteristic feature of the polymorph **3a** with an extended π-stacked structure, is not detected at cryogenic temperatures (77 K). We noted that the polymorph **3b** and the bimetallic Pt−Ag complexes **4** and **5**, which can be considered to form only π-stacked dimers in the solid state, do not show any low $\pi\pi$* excimeric emission. It must be mentioned that the X-ray structural analysis of the polymorph **3a**, commented before in the structural discussion, was carried out at 173 K. Therefore, to elucidate if on cooling there is a relationship between any structural change and the absence of the orange luminescence for **3a**, we have also carried out the structural X-ray analyses of **3a** at 293 and 100 K. Notwithstanding, no symmetry change has been observed in the entire range of temperatures, with maintenance of the $\pi\cdots\pi$ extended packing of the anions even at 100 K, and only the expected contraction of the unit cell was found on cooling. Although the metal−metal and $\pi\cdots\pi$ stacking distances become slightly shorter on decreasing the temperature (see Table S1 and Figure S4 in the SI for a comparison), practically all of them are equal within experimental error. Thus, the appearance of the orange emission when the temperature increases is tentatively attributed to the existence of a fast intersystem crossing from high-energy ^{3}LC/^{3}MLCT emissive states to the low-energy $^3\pi\pi$* excimeric manifold.

Conclusions

A new cyclometalated anionic derivative, $(NBu_4)[Pt(bzq)(C_6Cl_5)_2]$ (**2**), has been prepared, and its properties (absorption and emission) were compared with those of the related $(NBu_4)[Pt(bzq)(C_6F_5)_2]$ (**1**). The reactivity of **1** and **2** toward the Ag(I) ion has allowed us to prepare three new complexes, $[NBu_4][\{Pt(bzq)(C_6F_5)_2\}_2Ag]$ (**3**) and $[\{Pt(bzq)(C_6X_5)_2\}Ag(PPh_3)]$ (X = F (**4**), Cl (**5**)), stabilized by Pt→Ag donor−acceptor bonds and η^1-C(orthometalated)−Ag bonding interactions, confirmed by X-ray diffraction. For complex **3**, two different polymorphs were obtained from acetone/*n*-hexane, exhibiting visibly different luminescences (**3a** orange, λ_{max} 568 nm; **3b** green, λ_{max} 510 nm) at room temperature. The crystal structures of both of the anions (**3a** monoclinic, **3b** triclinic) are different, not only in their form, with a different conformation of the platinum planes (*anti* and planar **3a**, staggered and nonplanar **3b**), but also in terms of packing. Analysis of the **3a** crystal packing reveals the presence of an extended structure formed by $\pi\cdots\pi$ stacking interactions (∼3.6 Å) of the bzq ligands, whereas in **3b** two trimetallic Pt_2Ag anions form a dimer $(PtAgPt)_2$ by involving only two bzq ligands in $\pi\cdots\pi$ intermolecular interactions. The unstructured and broad, low-energy emission at 568 nm exhibited by **3a** at 298 K is attributed to a $\pi\pi$* excimeric emission, while the vibronic high-energy component with maxima at 510 and 534 nm is believed to be due to **3b** (mixed ^{3}LC/MLCT origin). At 77 K, the orange low energy is not detected and only a structured, green (λ_{max} 512 nm) emission due to ^{3}LC with some degree of ^{3}MLCT is observed.

For the bimetallic complexes **4** and **5**, the presence of the Pt→Ag donor−acceptor bond decreases the electronic density at the Pt center, causing a remarkable blue shift in the low-energy absorption when compared to the precursors, and also produces a sharp increase in the emission intensity. At room temperature in the solid, and in frozen CH_2Cl_2 solutions, the highly structured emission spectra of both complexes are identical, suggesting luminescence from states of a primarily ^{3}LC character, with a negligible contribution of the Pt−Ag bond. However, in contrast to the precursors, upon cooling the solid at 77 K, two different structured emissions with a short (12.4 μs for **4**, ∼21.2 μs for **5**) and a long (∼278 μs for **4**, 206 μs for **5**) lifetime are clearly resolved, being tentatively attributed to a ^{3}MLCT and a $\pi\pi$*(^{3}LC) emissive state, respectively.

Experimental Section

General Comments. Literature methods were used to prepare the starting materials $[NBu_4][Pt(C_6Cl_5)_3(tht)]$[71] and $[NBu_4][Pt(bzq)-$

(71) Usón, R.; Forniés, J.; Tomás, M.; Ara, I.; Menjón, B. *J. Organomet. Chem.* **1987**, *336*, 129.

$(C_6F_5)_3$].[38] C, H, and N analyses and mass, IR, and NMR spectra were performed as described elsewhere.[38] Molar conductances were carried out on a Philips PW9509 conductimeter in acetone and dichloromethane solutions (5×10^{-4} M). The optical absorption spectra were recorded using a Hewlett-Packard 8453 (solution) spectrophotometer in the visible and near-UV ranges. Emission and excitation spectra were obtained on a Perkin-Elmer LS 50B luminescence spectrometer and on a Jobin-Ybon Horiba Fluorolog 3-22 Tau-3 spectrofluorimeter, with the lifetime measured in phosphorimeter mode.

Safety Note: Perchlorate salts of metal complexes with organic ligands are potentially explosive. Only small amounts of material should be prepared, and these should be handled with great caution.

Preparation of [NBu_4][Pt(bzq)(C_6Cl_5)$_2$] (2). To a solution of [NBu_4][Pt(C_6Cl_5)$_3$(tht)] (0.300 g, 0.223 mmol) in toluene (10 mL) was added Hbzq (0.084 g, 0.471 mmol). After 6 h of reflux the existence of a green solid was observed. This solid was then filtered off, washed with ^{i}PrOH and *n*-hexane, and finally air-dried (0.080 g, 30% yield). Anal. Found: C, 43.85; H, 4.46; N, 2.56. $C_{41}H_{44}Cl_{10}N_2Pt$ requires: C, 44.17; H, 3.98; N, 2.51. IR (KBr): ν = 822 (m, C_6Cl_5, X-sensitive vibr.).[72] ^{1}H NMR (acetone-d_6, rt): 0.84 (t, 12H, ($N(CH_2CH_2CH_2CH_3)^+$), 1.31 (sext., 8H, ($N(CH_2CH_2CH_2$-$CH_3)^+$), 1.67 (m, 8H, ($N(CH_2CH_2CH_2CH_3)^+$), 3.29 (m, 8H, ($N(CH_2$-$CH_2CH_2CH_3)^+$), 6.94 (dd, 1H, J(^{195}Pt−H) = 40.8 Hz), 7.17 (t, 1H), 7.33 (m, 2H), 7.50 (d, 1H), 7.63 (d, 1H), 8.34 (dd, 1H), 7.94 ppm (dd, 1H, J(^{195}Pt−H) = 24.0 Hz).

Preparation of [NBu_4][{Pt(bzq)(C_6F_5)$_2$}$_2$Ag] (3). To a yellow solution of [NBu_4][Pt(bzq)(C_6F_5)$_2$] (0.050 g, 0.053 mmol) in acetone (6 mL) was added $AgClO_4$ (0.005 g, 0.026 mmol). After 1 h of stirring in the absence of light the solution was concentrated to ca. 3 mL, and a layer on *n*-hexane was deposited above. Slow diffusion of this *n*-hexane into the concentrated solution gave yellow crystals. These crystals were filtered off and air-dried, allowing evaporation of the crystallization solvents (0.017 g, 37% yield). Anal. Found: C, 44.89; H, 3.02; N, 2.40. $C_{66}H_{52}AgF_{20}N_3Pt_2$ requires: C, 44.91; H, 2.97; N, 2.38. IR (Nujol): ν = 1632 (w), 1562 (w), 1495 (s), 1057 (s), 1043 (m), 955 (s), 888 (w), 831 (m), 820 (w), 800 (m, C_6F_5, X-sensitive vibr.),[72] 777 cm^{-1} (m, C_6F_5, X-sensitive vibr.).[72] ^{1}H NMR (CD_2Cl_2, rt): 1.00 (t, 12H, ($N(CH_2CH_2CH_2CH_3)^+$), 1.45 (m, 8H, ($N(CH_2CH_2CH_2CH_3)^+$), 1.81 (m, 8H, ($N(CH_2CH_2CH_2$-$CH_3)^+$), 3.44 (m, 8H, ($N(CH_2CH_2CH_2CH_3)^+$), 7.02 (b, 4H), 7.31 (dd, 2H), 7.55 (m, 6H), 8.26 (dd, 2H, J(^{195}Pt−H) = 27.5 Hz), 8.51 ppm (dd, 2H). ^{19}F NMR (CD_2Cl_2, rt): −112.1 (b, 1F, *o*-F), −114.5 (b, 1F, *o*-F), −115.3 (d, 1F, *o*-F), −116.4 (m, 2F, *o*-F), −116.6 (b, 1F, *o*-F), −118.2 (d, 1F, *o*-F), −118.6 (d, 1F, *o*-F), −164.5 (m, 4F, *m*-F + *p*-F), −165.4 ppm (m, 3F, *m*-F + *p*-F), −166.0 ppm (m, 3F, *m*-F + *p*-F), −166.4 ppm (m, 2F, *m*-F). ^{19}F NMR (acetone-d_6, rt): −113.2 (b, 4F, *o*-F, J(^{195}Pt−F) = 546.7 Hz), −115.5 (b, 4F, *o*-F, J(^{195}Pt−F) = 314.0 Hz), −164.8 (m, 6F, *m*-F + *p*-F), −166.2 ppm (m, 6F, *m*-F + *p*-F).

Preparation of [{Pt(bzq)(C_6F_5)$_2$}Ag(PPh_3)] (4). To a yellow solution of [NBu_4][Pt(bzq)(C_6F_5)$_2$] (0.200 g, 0.210 mmol) in CH_2Cl_2 (30 mL) was added [Ag($OClO_3$)(PPh_3)] (0.099 g, 0.210 mmol). After 1 h of stirring in the absence of light the solution was evaporated to dryness. The residue was treated with OEt_2 (20 mL), and a white solid (NBu_4ClO_4) was filtered off. The yellow solution was evaporated to dryness, and the residue was treated with *n*-hexane, filtered off, and finally air-dried (0.175 g, 77% yield). Anal. Found: C, 47.66; H, 2.26; N, 1.37. $C_{43}H_{23}AgF_{10}NPPt$ requires: C, 47.93; H, 2.15; N, 1.30. IR (Nujol): ν = 1632 (w), 1500 (s), 1098 (m), 1060 (s), 1044 (m), 955 (s), 836 (m), 821 (w), 801 (m, C_6F_5, X-sensitive vibr.),[72] 777 (m, C_6F_5, X-sensitive vibr.),[72] 742 (s), 692 (s), 522 (m), 505 cm^{-1} (m). ^{1}H NMR ($CDCl_3$, rt): 6.94 (m, 7H), 7.28 (m, 10H), 7.41 (m, 2H), 7.63 (d, 1H), 7.81 (d, 1H), 8.35 (d, 1H), 8.70 ppm (d, 1H, J(^{195}Pt−H) = 21.6 Hz). ^{1}H NMR ($CDCl_3$, −60°C): 6.98 (m, 6H), 7.44 (m, 6H), 7.47 (m, 4H), 7.58 (t, 1H), 7.72 (m, 2H), 7.80 (d;1H), 8.37 (d, 1H), 8.64 ppm (d, 1H). ^{19}F NMR ($CDCl_3$, rt): −115.2 (d, 2F, *o*-F, J(^{195}Pt−F) = 538.3 Hz), −118.4 (d, 2F, *o*-F, J(^{195}Pt−F) = 344.0 Hz), −161.8 (t, 1F, *p*-F), −163.8 (m, 3F, *m*-F + *p*-F), −163.8 ppm (m, 2F, *m*-F). ^{19}F NMR ($CDCl_3$, −60 °C): −113.8 (d, 1F, *o*-F, J(^{195}Pt−F) = 597.6 Hz), −116.0 (d, 1F, *o*-F, J(^{195}Pt−F) = 378.7 Hz), −118.9 (d, 2F, *o*-F, J(^{195}Pt−F) = 313.8 Hz), −161.9 (t, 1F, *p*-F), −163.1(m, 3F, *m*-F + *p*-F), −164.5 ppm (m, 2F, *m*-F). ^{31}P NMR ($CDCl_3$, −60 °C): 13.0 ppm (J(^{109}Ag−P) = 733.3, J(^{107}Ag−P) = 637.8, J(^{195}Pt−P) = 228 Hz).

Preparation of [{Pt(bzq)(C_6Cl_5)$_2$}Ag(PPh_3)] (5). To a yellow solution of [NBu_4][Pt(bzq)(C_6Cl_5)$_2$] (0.080 g, 0.007 mmol) in CH_2Cl_2 (15 mL) was added [Ag($OClO_3$)(PPh_3)] (0.034 g, 0.072 mmol). After 1 h of stirring in the absence of light the solution was evaporated to dryness. The residue was treated with OEt_2 (15 mL), and a white solid (NBu_4ClO_4) was filtered off. The yellow solution was evaporated to dryness, and the residue was treated with *n*-hexane, filtered off, and finally air-dried (0.026 g, 29% yield). Anal. Found: C, 41.56; H, 1.82; N, 0.90. $C_{43}H_{23}AgCl_{10}NPPt$ requires: C, 41.58; H, 1.87; N, 1.13. IR (KBr): ν = 1622 (w), 1479 (m), 1435 (s), 1326 (s), 1315 (s), 1289 (vs), 1261 (m), 1213 (s), 1097 (vs), 833 (s), 819 (m, C_6Cl_5, X-sensitive vibr.),[72] 741 (s), 722 (m), 692 (s), 671 (s), 624 (m), 5,21 (s), 508 cm^{-1} (m). ^{1}H NMR (acetone-d_6, rt): 6.66 (m, 6H), 7.16 (m, 6H), 7.34 (m, 5H), 7.44 (dd, 1H), 7.54 (d, 1H), 7.66 (d, 1H), 7.69 (d, 1H), 8.32 (dd, 1H), 8.56 ppm (dd, 1H, J(^{195}Pt−H) = 16.4 Hz). ^{31}P NMR (acetone-d_6, rt): 10.4 ppm (J(^{109}Ag−P) = 727.0, J(^{107}Ag−P) = 635.0, J(^{195}Pt−P) = 236 Hz).

X-ray Structure Determinations. Crystal data and other details of the structure analyses are presented in Table 5 (full data for the X-ray analyses of **3a** at 100 and 293 K are presented in the SI). Suitable crystals for X-ray diffraction studies were obtained by slow diffusion of *n*-hexane into concentrated solutions of the complexes in 3 mL of Me_2CO (**3a** and **3b**) or $CHCl_3$ (**4**·$CHCl_3$·0.5*n*-C_6H_{14} and **5**·0.58$CHCl_3$·0.25*n*-C_6H_{14}). Crystals were mounted at the end of a quartz fiber. The radiation used in all cases was graphite-monochromated Mo Kα (λ = 0.71073 Å).

For **3a** and **3b**, X-ray intensity data were collected with a Nonius κCCD area-detector diffractometer. Images were processed using the DENZO and SCALEPACK suite of programs.[73] The absorption correction was performed using SORTAV.[74] For **4**·$CHCl_3$·0.5*n*-C_6H_{14}, X-ray intensity data were collected on a Bruker Smart Apex diffractometer. The diffraction frames were integrated using the SAINT program.[75] For **5**·0.58$CHCl_3$·0.25*n*-C_6H_{14}, X-ray intensity data were collected on an Oxford Diffraction Xcalibur diffractometer. The diffraction frames were integrated using the CrysAlis RED program.[76] Both sets of data were corrected for absorption with SADABS.[77]

The structures were solved by Patterson and Fourier methods and refined by full-matrix least squares on F^2 with SHELXL-97.[78] All non-hydrogen atoms were assigned anisotropic displacement parameters and refined without positional constraints, except as noted below. All hydrogen atoms were constrained to idealized geometries and assigned isotropic displacement parameters equal to 1.2 times the U_{iso} values of their attached parent atoms (1.5 times for the methyl hydrogen atoms). In the structure of **5**·0.58$CHCl_3$·0.25*n*-C_6H_{14}, a $CHCl_3$ and half an *n*-hexane molecule were found

(72) Maslowsky, E. J. *Vibrational Spectra of Organometallic Compound*; Wiley: New York, 1977.

(73) Otwinowski, Z.; Minor, W. *Methods Enzymol. A: Macromol. Crystallogr.* **1997**, *276*, 307.

(74) Blessing, R. H. *Acta Crystallogr., Sect. A* **1995**, *51*, 33.

(75) *SAINT*; Siemens Analytical X-ray Instruments Inc: Madison, WI, 1994.

(76) *CrysAlis RED*; Oxford Diffraction: Oxford, UK, 2004.

(77) Sheldrick, G. M. *SHELXL-94*; University of Göttingen: Germany, 1994.

(78) Sheldrick, G. M. *SHELXL-97*; University of Gottingen: Germany, 1997.

Table 5. Crystal Data and Structure Refinement for 3a, 3b, 4·$CHCl_3$·0.5*n*-C_6H_{14}, and 5·0.58$CHCl_3$·0.25*n*-C_6H_{14}

	3a	3b	4	5
empirical formula	$C_{66}H_{52}AgF_{20}N_3Pt_2$	$C_{66}H_{52}AgF_{20}N_3Pt_2$	$C_{43}H_{23}AgF_{10}NPPt \cdot CHCl_3 \cdot 0.5n\text{-}C_6H_{14}$	$C_{43}H_{23}AgCl_{10}NPPt \cdot 0.58CHCl_3 \cdot 0.25n\text{-}C_6H_{14}$
fw	1765.16	1765.16	1240.01	1333.23
temp/K	173(1)	123(1)	100(1)	100(1)
wavelength/Å	0.71073	0.71073	0.71073	0.71073
cryst syst	monoclinic	triclinic	triclinic	trigonal
space group	$P2_1/c$	$P\bar{1}$	$P\bar{1}$	$P\bar{3}$
a/Å	15.6840(2)	10.6672(2)	12.7520(5)	25.0431(4)
b/Å	18.6779(2)	15.5158(3)	13.0864(6)	25.0431(4)
c/Å	20.5826(3)	20.2547(5)	13.5349(6)	13.0989(2)
α/deg	90	107.523(1)	96.672(1)	90
β/deg	91.1239(4)	91.395(1)	93.068(1)	90
γ/deg	90	108.458(1)	103.451(1)	120
vol/Å^3	6028.39(13)	3005.69(11)	2174.24(16)	7114.46(14)
Z	4	2	2	6
calc dens/g cm^{-3}	1.945	1.950	1.894	1.867
abs coeff/mm^{-1}	5.059	5.073	3.964	4.090
θ range/deg	1.3−25.0	2.7−25.0	1.5−25.0	4.0−25.1
data collected	77715	10573	11932	45574
indep data (R_{int})	10 612 (0.0667)	10 573 (0)	7564 (0.0142)	8387 (0.0265)
no. of data/restraints/params	10 612/0/829	10 573/1/832	7564/0/577	8387/3/554
GOF on F^2 [a]	1.003	1.054	1.013	1.051
final R^b indices [$I > 2\sigma(I)$]	R1 = 0.0332, wR2 = 0.0868	R1 = 0.0332, wR2 = 0.0592	R1 = 0.0248, wR2 = 0.0621	R1 = 0.0338, wR2 = 0.0863
R^b indices (all data)	R1 = 0.0550, wR2 = 0.1152	R1 = 0.0490, wR2 = 0.0641	R1 = 0.0265, wR2 = 0.0628	R1 = 0.0363, wR2 = 0.0877

[a] Goodness-of-fit = $[\sum w(F_o^2 - F_c^2)^2 / (N_{obs} - N_{param})]^{0.5}$. [b] $R1 = \sum(|F_o| - |F_c|)/\sum|F_o|$. [c] $wR2 = [\sum w(F_o^2 - F_c^2)^2/\sum w(F_o^2)^2]^{0.5}$.

lying in the same area and were refined with partial occupancy 0.25/0.25, respectively. Bond distance restraints were used for the atoms of this chloroform molecule. A difference Fourier map at the end of refinement shows what appear to be two local peaks with large densities (3.08, 2.98 e Å^{-3}) located in a channel running parallel to the crystallographic *z*-axis. Inspection of the contoured map (using Platon[79]) reveals that these are two local peaks in a large, diffuse area of electron density that shows other, smaller local maxima. Assignment of atomic sites to the two largest maxima did not lead to stable refinement, as would be expected from the characteristics of the actual contoured map. The results reported here are those obtained from a refinement in which these peaks were not assigned and with no further treatment of the data. Full-matrix least-squares refinement of these models against F^2 converged to final residual indices given in Table 5.

(79) Spek, A. L. *Platon*; Utrecht University: Utrecht, The Netherlands, 1998.

Acknowledgment. Financial support has been obtained from the Ministerio de Ciencia y Tecnología and FEDER (Project CTQ2005-08606-C02-01, 02) and the Diputación General de Aragón (Grupo de Excelencia). S.I. and J.T. thank the Ministerio de Educación y Ciencia and the CAR, respectively, for a grant.

Supporting Information Available: Emission spectra for complexes **1**, **2**, **4**, and **5** in frozen solution, for complex **5** in the solid state at 77 and 298 K, and for **3a** and **5** (with different delays) in the solid state at 77 K. Further details of the structure determinations of **3a** (also full details for the structural studies at 100 and 293 K), **3b**, **4**·$CHCl_3$·0.5*n*-C_6H_{14}, and **5**·0.58$CHCl_3$·0.25*n*-C_6H_{14} including atomic coordinates, bond distances and angles, and thermal parameters. This material is available free of charge via the Internet at http://pubs.acs.org.

OM0604526